WPEDU-PR(18) 21091

D Brunetti et al.

Excitation mechanism of low-n edge harmonic oscillations in ELM-free high performance tokamak plasmas

Preprint of Paper to be submitted for publication in
Physical Review Letters

This work has been carried out within the framework of the EUROfusion Consortium and has received funding from the Euratom research and training programme 2014-2018 under grant agreement No 633053. The views and opinions expressed herein do not necessarily reflect those of the European Commission.

Excitation mechanism of low-n edge harmonic oscillations in ELM-free high performance tokamak plasmas

D. Brunetti,[1,*] J. P. Graves,[2] E. Lazzaro,[1] A. Mariani,[1] S. Nowak,[1] W. A. Cooper,[2] and C. Wahlberg[3]

[1]Istituto di Fisica del Plasma IFP-CNR, Via R. Cozzi 53, 20125 Milano, Italy
[2]École Polytechnique Fédérale de Lausanne (EPFL), Swiss Plasma Center (SPC), CH-1015 Lausanne, Switzerland
[3]Department of Physics and Astronomy, P.O. Box 516, Uppsala University, SE-751 20 Uppsala, Sweden

(Dated: September 6, 2018)

The excitation mechanism for low-n Edge Harmonic Oscillations in quiescent H-mode regimes is identified analytically. We show that the combined effect of diamagnetic and poloidal MHD flows leads to the stabilisation of short wavelength modes, allowing low-n perturbation to grow. The analysis, performed in tokamak toroidal geometry, includes the effects of large edge pressure gradients, associated with the local flattening of the safety factor and diamagnetic flows, sheared parallel and $\boldsymbol{E}\times\boldsymbol{B}$ rotation and a vacuum region between plasma and the ideal metallic wall. The separatrix also is modelled analytically.

Introduction.— Tokamak high-confinement (H-mode) regimes are attractive operating scenarios for fusion reactors because of their long energy confinement time [1]. The large edge pressure gradients, which characterise H-mode plasmas, favour the formation of short wavelength magnetohydrodynamic (MHD) perturbations called edge localised modes (ELMs) [2]. Rapid energy and particle expulsions are usually associated with ELMs. Though this can be beneficial for impurity control, ELMs deposit unacceptable peak heat loads on the divertor target causing a severe deterioration of the plasma facing components. This motivates a lively line of research focussed on the development of sustained high confinement regimes with intrinsically no ELMs.

One of the most promising high performance naturally ELM-free operating regimes is the so called quiescent high-confinement (QH) mode [3–5]. QH scenarios are usually observed at low edge collisionality ($\nu_e^* < 0.3$) over a fairly broad range in q_{95} ($3 \lesssim q_{95} \lesssim 6$) [6, 7]. At low ν_e^*, large edge pressure gradients are associated with a significant bootstrap contribution to the current. In QH plasmas ELMs are suppressed and replaced by low-n steady mild MHD perturbations called edge harmonic oscillations (EHOs). These have been observed in DIII-D [4, 6–8], ASDEX-U [5, 9], JET [10], and JT60 [11]. The edge particle transport is enhanced by EHOs, thus allowing density control and potentially ash removal without the impulsive heat load problem [6, 12]. EHOs are dominantly low-n perturbations (usually $n \sim 1, 2$) accompanied by weaker higher-n modes up to $n \sim 10$ [5, 7, 8]. A single EHO harmonic n rotates with frequency $n\Omega_{ped}$ (Ω_{ped} is the plasma toroidal rotation frequency at the pedestal top) [3, 10, 13].

The excitation mechanism of such instabilities is still unclear. Previous theoretical interpretations suggested that short wavelength modes exhibiting *infernal* features [13–16], though dominant in the linear phase, were suppressed nonlinearly and superseded by steady low-n modes [17, 18] with no significant effects of the parallel flow [17, 19]. Recent experimental findings point to the $\boldsymbol{E}\times\boldsymbol{B}$ shearing rate as the key ingredient for the development of the characteristics of these oscillations [19]. Indeed numerical investigations of QH-mode DIII-D plasma discharges with sheared $\boldsymbol{E}\times\boldsymbol{B}$ flows showed that low-n modes are linearly dominant and are eventually sustained in the nonlinear stage at moderately low amplitude [7, 20–24].

In this Letter the specific physical mechanisms which allow low-n EHOs to emerge are identified by extending the analysis of Ref. [25] within the *infernal model* framework. Our new analytic work, focusses on the linear stability of moderately low-n ideal modes with the inclusion of toroidal effects and toroidal and poloidal flows (both MHD and diamagnetic). It shows that short wavelength modes are entirely suppressed. Hence the linear calculations show that ELM free H-mode regimes are established by robustly preventing infinitesimally small amplitude short wavelength modes.

Physical model.— Let us analyse small inverse aspect ratio tokamak geometry ($\varepsilon = a/R_0 \ll 1$ where R_0 and a are the major and minor radii respectively), with shifted circular toroidal surfaces. We consider a low-$\beta = 2\mu_0 p/B_{ax}^2 (\sim \varepsilon^2)$ plasma, where p is the pressure and B_{ax} the magnetic field strength on the axis. A right handed straight field line coordinate system (r, ϑ, φ) is introduced where r is a flux label with the dimensions of length, ϑ (counter-clockwise in the poloidal plane) and φ are the poloidal-like and toroidal angles respectively with contravariant basis vectors $(\boldsymbol{\nabla} r, \boldsymbol{\nabla}\vartheta, \boldsymbol{\nabla}\varphi)$. We assume that additional effects (i.e. non-static or beyond MHD, e.g diamagnetic) do not alter to leading order of the standard static equilibrium (whose associated metric tensor coefficients can be found in Ref. [26]). The equilibrium magnetic field in the plasma is $\boldsymbol{B} = T\boldsymbol{\nabla}\varphi - \boldsymbol{\nabla}\psi\times\boldsymbol{\nabla}\varphi$ where ψ is the poloidal flux.

The plasma is described by the ideal drift-MHD equations [27]:

$$\rho\left(d_t\boldsymbol{v} + \boldsymbol{v}^*\cdot\boldsymbol{\nabla}\boldsymbol{v}_\perp\right) = -\boldsymbol{\nabla}p + \boldsymbol{J}\times\boldsymbol{B}, \tag{1}$$

$$\partial_t\boldsymbol{B} = \boldsymbol{\nabla}\times(\boldsymbol{v}\times\boldsymbol{B}), \tag{2}$$

$$\partial_t p + \boldsymbol{v}\cdot\boldsymbol{\nabla}p + \Gamma p\boldsymbol{\nabla}\cdot\boldsymbol{v}_i = 0, \quad \partial_t\rho + \boldsymbol{\nabla}\cdot(\rho\boldsymbol{v}_i) = 0, \tag{3}$$

where $d_t = \partial_t + \boldsymbol{v}\cdot\boldsymbol{\nabla}$, $\boldsymbol{v}$ and $\boldsymbol{v}^* = m_i\boldsymbol{B}\times\boldsymbol{\nabla}p/(e\rho B^2)$ (m_i is the ion mass) are the plasma MHD and ion diamagnetic velocities respectively with $\boldsymbol{v}_i = \boldsymbol{v} + \boldsymbol{v}^*$, ρ is mass density, $\boldsymbol{J} = \boldsymbol{\nabla}\times\boldsymbol{B}$ the current density (having normalised $\mu_0 = 1$), p

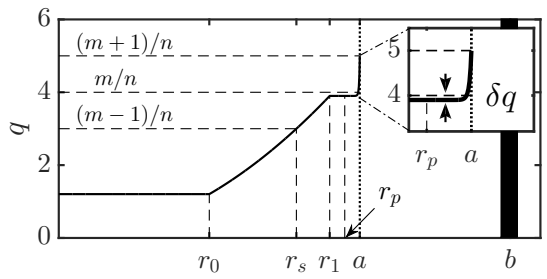

Figure 1. Example of a model safety factor profile employed in our analysis. Note the $(m+1)/n$ resonance at the plasma boundary mimicking the separatrix.

the pressure and $\Gamma = 5/3$ is the adiabatic index. The symbol $\perp$ indicates the vector perpendicular projection to the magnetic field, i.e. $\boldsymbol{v}_\perp = \boldsymbol{B}\times(\boldsymbol{v}\times\boldsymbol{B})/B^2$. The Faraday-Ohm's law has been approximated within the limit of nearly isothermal ions ($T_i \approx const$) [10, 28] and small plasma compressibility.

In choosing the equation for the pressure evolution, it has been implicitly assumed that T_i significantly exceeds T_e so that $p_0 \approx p_{0i}$. Moreover, by assuming that T_e is proportional to ρ at equilibrium and that the perturbations of the mass density and the electron temperature are dominated mainly by convection (i.e. the $\boldsymbol{v}\cdot\boldsymbol{\nabla}$ term), we obtain that the perturbed pressure is given by the ion contribution.

The rotational transform profile (denoted with μ with $q = 1/\mu$) is piecewise continuous [25], constant for $0 < r < r_0$ and $r_1 < r < r_p$ ($r_p = (r_1 + a)/2$), with values μ_{ax} and μ_1 respectively ($\mu_{ax} > \mu_1 = 1/(m/n - \delta q)$), while $\mu = \mu_1(r_1/r)^2$ for $r_0 < r < r_1$. The separatrix is modelled by imposing for $r_p < r < a$ a narrow region of high magnetic shear :

$$(m+1)\mu - n = S\,[1-(r/a)^\lambda], \quad \lambda \to \infty, \tag{4}$$

where S is a constant such that $\mu(r_p) = \mu(r_1)$ (note that for $\lambda \to \infty$ this high shear region becomes infinitesimally narrow so that we regard the region $r_* < r < a$ as shear-free). A *vacuum region* between plasma and the ideally conducting wall extends from $r = a$ to $r = b$ (the wall thickness is irrelevant). We refer to the regions $0 < r < r_1$ and $a < r < b$ as the *outer regions*, while the region $r_1 < r < a$ is the *pedestal region* (the q profile and the relevant radial positions are shown in Fig. 1).

An equilibrium helical MHD flow ($v_0^r = 0$, $v_0^\vartheta = \omega_p(r)$ and $v_0^\varphi = \Omega(r)$ [29]) is assumed. Such a flow is sufficiently weak so that the centrifugal corrections to equilibrium pressure and mass density profiles [30] are negligible within the approximations employed in this work [15]. Equilibrium flow and mass density (pressure) gradients are localised within the *pedestal region*. Equilibrium quantities are denoted by the subscript 0 while perturbed ones, denoted by a tilde, have a time dependence of the type $e^{i\gamma t}$ (γ complex).

Eigenmode equations.— The *infernal* model [31, 32] assumes the presence of three poloidal Fourier harmonics, one dominant (m) coupled to two neighbouring sidebands ($m \pm 1$). Hence we write the perturbed velocity as $\tilde{\boldsymbol{v}} = \tilde{\boldsymbol{v}}_m(r)e^{i[m\vartheta - n\varphi]} + \sum_{m'=\pm1}\tilde{\boldsymbol{v}}_{m+m'}(r)e^{i[(m+m')\vartheta - n\varphi]}$ with $\tilde{\boldsymbol{v}}_{m\pm1} \sim \varepsilon\tilde{\boldsymbol{v}}_m$ (since n is fixed, we omit to specify the toroidal mode number in writing the Fourier components). Mode coupling, induced by the metric oscillation of the Jacobian, is favoured in presence of large pressure gradients and field line bending weakening (i.e. weak shear).

In the *inner* and *outer* regions, because of field line bending dominating over inertia and vanishing pressure gradients, different poloidal Fourier harmonics behave independently according to [25, 33] (here $\ell = m, m\pm1$ and $' \equiv d/dr$):

$$\left[r^3(\ell\mu - n)^2\xi_\ell'\right]' - r(\ell^2-1)(\ell\mu-n)^2\xi_\ell = 0, \tag{5}$$

having introduced the Lagrangian-like radial fluid displacement $\xi_\ell = \tilde{v}_\ell^r/\gamma_\ell$ with $\gamma_\ell = \gamma + i\ell\omega_p - in\Omega$ [34].

The main difficulty is to derive the eigenmode equation for the mth harmonic, which contains the inertial contributions due to $\boldsymbol{E}\times\boldsymbol{B}$ and diamagnetic flows. In the pedestal region we impose the ordering $\delta q/q \sim \varepsilon$ and $\gamma/m \sim \Omega \sim \omega_p \sim \omega^* \sim \varepsilon\omega_A$ where $\omega^*(r) = \boldsymbol{v}_0^*\cdot\boldsymbol{\nabla}\vartheta$ and $\omega_A = B_{ax}/(R_0\sqrt{\rho_0})$ (the Alfvén frequency with B_{ax} the magnetic field equilibrium value on the axis). To leading order the $\frac{1}{R^2}\boldsymbol{\nabla}\varphi$ projection of (1) yields $\tilde{B}^\varphi = 0$. From the contravariant radial, poloidal and toroidal projections of (2) we obtain respectively $(\sqrt{g}\tilde{B}^r)_\ell = ir(\ell\mu - n)\xi_\ell$, $\frac{1}{r}(r\tilde{v}_m^r)' + im\tilde{v}_m^\vartheta - in\tilde{v}_m^\varphi = 0$ and $\tilde{v}_m^\varphi + \Omega'\xi_m = 0$. It follows that $(\sqrt{g}\tilde{B}^\vartheta)_m = -\frac{1}{im}(\sqrt{g}\tilde{B}^r)'_m$ and $\tilde{B}_m^i \sim \tilde{B}_{m\pm1}^i$. We point out that in case of large radial gradients and poloidal wave numbers the relations above still hold. The perturbed pressure is written in terms of ξ according to $\tilde{p}_\ell = -p_0'\xi_\ell + \delta p_\ell$, where δp is the *non-convective* contribution. In the limit $T_i \approx const$ with δp small, we have $\tilde{\boldsymbol{v}}^* \simeq \frac{\boldsymbol{\nabla}\varphi}{eB_0^\varphi}\times\boldsymbol{\nabla}\left(\frac{\tilde{p}}{n_0}\right)$ (n_0 is the equilibrium numerical density).

One of the key ingredients of our analysis is the smallness of the poloidal ion flow in the pedestal region [19, 35, 36]:

$$\omega_p + \omega^* \approx 0. \tag{6}$$

Further simplification is achieved by assuming that large radial gradients are localised within a narrow region, hence:

$$rd\ln f/dr \gg 1, \quad f = \xi_\ell, \rho_0, p_0, \Omega, \omega_p.$$

In addition we assume $m \gg 1$ (and so $n = m/q$ with $q \sim 1$).

The equation for the generic radial displacement ξ_ℓ is obtained by applying the operator $\sqrt{g}\boldsymbol{\nabla}\varphi\cdot\boldsymbol{\nabla}\times 1/B_0^\varphi (\equiv \mathbf{D})$ on the perturbed momentum equation [37, 38], and then selecting the ℓth Fourier component. Field line bending dominates over inertia in the sidebands equations (modes with poloidal mode number $m \pm 1$), so that additional flow effects play no role in their corresponding eigenmode equations which read [25]:

$$\left(r^{2\pm m}\xi_{m\pm1}\right)' = r^{1\pm2m}L_\pm + \tfrac{1\pm m}{2}\alpha r^{1\pm m}\xi_m, \tag{7}$$

where $L_\pm$ are constants of integration which are determined later. Focussing on the mth harmonic, at leading order a rather

lengthy but straightforward algebra gives (the cylindrical limit proves to be sufficient):

$$\left[\mathbf{D}[\widetilde{\rho\,(d_t\boldsymbol{v}+\boldsymbol{v}^*\cdot\boldsymbol{\nabla}\boldsymbol{v}_\perp)}]\right]_m=\frac{i}{mR_0}\left[r^2\,(K\xi_m')'-m^2K\xi_m\right],$$

with $K=\gamma_D(\gamma_D+im\omega_p)/\omega_A^2$ and $\gamma_D=\gamma-in\Omega$ having normalised $B_{ax}=1$. Exploiting the metric oscillation in the Jacobian it is easy to see that $[\mathbf{D}(\boldsymbol{\nabla}\delta p)]_m\approx ir(\delta p_{m+1}-\delta p_{m-1})'+im(\delta p_{m+1}+\delta p_{m-1})$. We take the limit $\widetilde{(p\boldsymbol{\nabla}\cdot\boldsymbol{v}_i)}\to 0$ by keeping $\Gamma\widetilde{(p\boldsymbol{\nabla}\cdot\boldsymbol{v}_i)}$ finite [38–40], which yields $\tilde v^\varphi_{m\pm1}+\Omega'\frac{\tilde v^r_{m\pm1}}{\gamma_{m\pm1}}\simeq-\frac{r}{R_0}\tilde v^\varphi_m-\frac{q}{imR_0}\left[r(\gamma_D\xi_m)'\mp\gamma_D\xi_m\right]$. From the perturbed $\boldsymbol{B}/B_0^2$ ($B_0=|\boldsymbol{B}_0|$) projection of Eq. (1) we get $\delta p_{m\pm1}=\pm\frac{q^2K}{mR_0}\,(r\xi_m'\mp m\xi_m)$, and thus:

$$[\mathbf{D}(\boldsymbol{\nabla}\delta p)]_m=\frac{2q^2i}{mR_0}\left[r^2(K\xi_m')'-m^2K\xi_m\right],$$

which embodies the Glasser-Greene-Johnson inertia enhancement factor [41]. To leading order we have $\tilde p_m\approx-p_0'\xi_m$, so that the poloidal covariant projection of (1) yields $\tilde B_\varphi\approx R_0p_0'\xi_m$. Hence with $(\delta q/q)a\frac{d}{dr}\sim1$ and $-2R_0p_0'q^2=\alpha\sim1$ it follows that [31]:

$$[\mathbf{D}(\boldsymbol{\nabla}(p_0'\xi)+\widetilde{\boldsymbol{J}\times\boldsymbol{B}})]_m=-\frac{in^2}{mR_0}\Big[\left(\tfrac{\delta q}{q}\right)^2(r^2\xi_m''-m^2\xi_m)$$
$$-\frac{\alpha^2}{2}\xi_m+\frac{\alpha}{2}\sum\tfrac{r^{-1\mp m}}{1\pm m}\left(r^{2\pm m}\xi_{m\pm1}\right)'\Big].$$

Thus collating these results together and eliminating the sideband displacements $\xi_{m\pm1}$ in the equation above by means of (7), the eigenmode equation for the main harmonic ξ_m in the *pedestal region* finally reads [25, 31]:

$$r^2\,(Q\xi_m')'-m^2Q\xi_m+\tfrac{\alpha}{2}\sum\tfrac{r^{\mp m}L_\pm}{1\pm m}=0,\qquad(8)$$

where $Q=(1+2q^2)K/(n^2\omega_A^2)+(\delta q/q)^2$. Equations (5), (7) and (8) form the basis four our analysis.

Dispersion relation.— We assume that the profiles of equilibrium mass density, pressure and toroidal rotation are steplike [25]:

$$p_0(r)/p_0(r_1)\sim\rho_0(r)/\rho_0(r_1)\sim\Omega(r)/\Omega(r_1)\sim\theta(r_p-r),$$

where $\theta(x)$ is the Heaviside step function of argument x. Since the poloidal MHD flow must cancel the diamagnetic flow (cf. (6) with $\omega^*\propto p_0'$), we choose ω_p of the form [42]:

$$\omega_p(r)=\omega_Er_p\delta(r-r_p)\Delta,$$

with $\Delta=(a-r_1)/r_p$ and ω_E constant. Note that $\int_{r_1}^a\omega_pdr/\int_{r_1}^a dr=\omega_E$.

Writing symbolically (8) as $(Q\xi_m')'+f(r)=0$ we define $F(r)=\int_{r_1}^r f(\hat r)d\hat r$ so that $Q\xi_m'+F(r)=C$ where C is a constant of integration. The function F is bounded, thus dividing the previous result by Q (supposed non-vanishing) and then integrating across r_p shows that ξ_m is continuous at r_p. The solutions of Eq. (5) in the region $0<r<r_1$ and $a<r<b$ for the dominant mode ξ_m provide the appropriate boundary conditions at r_1 and a, namely $\xi_m(r_1)=\xi_m(a)=0$ [25, 43]. Thus using the profiles for mass density, pressure, toroidal and poloidal MHD flows and solving (8) on the left and on the right of r_p with the boundary conditions at r_1 and a given above, we obtain to leading order:

$$\xi_m\propto\begin{cases}\dfrac{e^{mr/r_p}-e^{m(2r_1/r_p-r/r_p)}}{e^m-e^{m(2r_1/r_p-1)}}, & r<r_p,\\[2ex] \dfrac{e^{mr/r_p}-e^{m(2a/r_p-r/r_p)}}{e^m-e^{m(2a/r_p-1)}}, & r>r_p.\end{cases}$$

where the slowly varying terms in r have been approximated by setting $r\approx r_p$. Note that ξ_m is symmetric about r_p.

Now we must define the constants $L_\pm$. According to Ref. [25], with the equilibrium profiles given above, first equation (7) is evaluated at r_1 and a providing respectively $\xi_{m\pm1}(r_1)$ and $\xi_{m\pm1}(a)$ (both functions of $L_\pm$). Then, plugging these expressions into Eq. (7) and integrating from r_1 to a gives $\frac{r_p^{\pm m}L_\pm}{1\pm m}=\xi_m\frac{\beta_1q^2}{\varepsilon_p}\Lambda^{(\pm)}$, where $\beta_1=2p_0(r_1)$, $\varepsilon_p=r_p/R_0$ and [25, 32]:

$$\Lambda^{(\pm)}=\frac{(r_p/r_1)^{2\pm2m}(1\pm m)[2\pm m+\mathbb{C}_\pm][2\pm m+\mathbb{B}_\pm]}{(\mathbb{C}_\pm\mp m)[2\pm m+\mathbb{B}_\pm]-(\mathbb{B}_\pm\mp m)[2\pm m+\mathbb{C}_\pm]\left(\frac{a}{r_1}\right)^{2\pm2m}},$$

with $\mathbb{C}_\pm\equiv[rd(\ln\xi_{m\pm1})/dr]_{r_1}$ and $\mathbb{B}_\pm\equiv[rd(\ln\xi_{m\pm1})/dr]_a$.

The quantities $\mathbb{C}_\pm$ are obtained by solving Eq. (5) in the region $0<r<r_1$ and thus imposing smooth matching of the sideband eigenfunctions $\xi_{m\pm1}$ across r_1 [25, 32]. The constant $\mathbb{B}_-$ is evaluated similarly (the vacuum perturbation obeys to (5) as well) with the replacement $r_1\to a$. These have been computed in Ref. [25] and for large m and small δq they read $\mathbb{C}_+\approx3m+2$, $\mathbb{C}_-\approx m/6-1/4$ and $\mathbb{B}_-\approx2-3m$ (in the latter expression we approximated $(a/b)^{2m-2}\to0$).

Finally $\mathbb{B}_+$ is obtained by solving equation (5) (which is equivalent to (7) for μ constant and $\alpha\to0$) for $r_p<r<a$ with μ given by (4). The solution for ξ_{m+1} can be expressed exactly in terms of the hypergeometric functions [26], so that forcing ξ_{m+1} to be finite at its own resonant surface and taking the limit $\lambda\to\infty$ yields:

$$\xi_{m+1}\propto(r/a)^{m-2}+(1-{}^2\!/_m)(r/a)^{-m},$$

from which $\mathbb{B}_+=0$. We point out that with an ideally conducting metallic wall directly interfaced with the plasma (i.e. $\mathbb{B}_\pm\to\infty$) the driving term $\Lambda^{(+)}+\Lambda^{(-)}$ is negative implying stability. Thus in the limit of large m and sufficiently far wall we may approximate $\Lambda^{(+)}=\frac{m(r_p/a)^{2m}}{1+1/2(r_1/a)^{2m}}$ and $\Lambda^{(-)}=\frac{2m(a/r_p)^{2m}}{1+3(a/r_1)^{2m}}$. The m upper boundary for which the approximations hold can be estimated by requiring $\frac{1}{m}rd\ln\xi_mr/dr|_{r_p}\gtrsim1$ (for the parameters which will be employed in the numerical evaluation of the growth rate we would take $m\sim40-50$).

Therefore by taking $\gamma_D=\gamma-in\Omega_1$ with $\Omega_1=\Omega(r_1)$, according to Refs. [25, 30] integration of (8) across r_p yields the

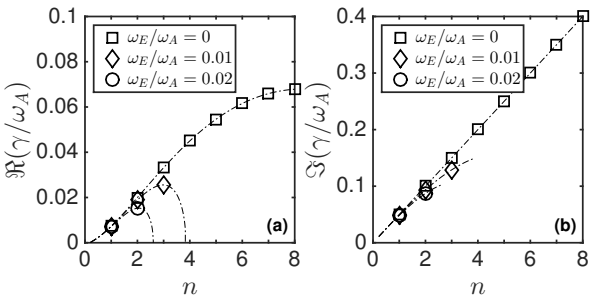

Figure 2. Real (a) and imaginary (b) parts of γ evaluated from Eq. (9) with $q \approx 5$, $\varepsilon = 1/3$, $r_1/a = 0.95$, $\Omega_1/\omega_A = 5 \times 10^{-2}$, $\beta_1 = 0.3\%$ and $\delta q = 0.1$.

dispersion relation which in the limit $q \gg 1$ reads:

$$\frac{\gamma}{n\omega_A} \approx i\left(\frac{\Omega_1}{\omega_A} - \frac{m^2 q \omega_E \Delta}{2\mathfrak{D}\omega_A}\right) + \sqrt{\frac{(\beta_1 q)^2 \Lambda}{4\mathfrak{D}\varepsilon_p^2} - \frac{\delta q^2}{q^4} - \left(\frac{m^2 q \omega_E \Delta}{2\mathfrak{D}\omega_A}\right)^2} \tag{9}$$

where $\Lambda = \Lambda^{(+)} + \Lambda^{(-)}$ and $\mathfrak{D} = m\coth[m(1 - r_1/r_p)]$ $=(rd\ln\xi_m/dr|_{r_p-\delta}$ with $\delta \to 0)$. Hereafter it is understood that ω_A is the value of the Alfvén frequency on the magnetic axis.

By setting $\omega_E = 0$ (viz. neglecting all poloidal flow corrections) we recover the dispersion relation derived in [25], whose features have been already extensively analysed (note that the only effect of toroidal rotation is to Doppler shift the eigenmode frequency). Indeed the first two terms under the sign of square root are the linear growth rate of the purely MHD perturbation. The imbalance in the inertial contribution of the Doppler correction to γ due to the combination of poloidal MHD and diamagnetic flows, produces the last term in the square root of (9). This term, although small for small m values, increases its amplitude with the poloidal (or equivalently the toroidal) mode number. Hence due to its interplay with the pressure ($\propto \beta$) and field line bending weakening ($\propto \delta q$) driving terms, allows the suppression of short wavelength perturbations favouring the growth of low n modes. This is shown in figure 2 where the real and imaginary parts of γ are computed by means of (9) with reactor relevant parameters. Finally we point out that the ω_E stabilisation mechanism is independent of mode coupling. Hence it may be expected that if a larger number of coupled harmonics is allowed, with the growth rate driving contribution increasing linearly with n [7, 20], such a stabilisation stills occurs.

Conclusions.— In this Letter the excitation mechanism for low-n EHOs has been identified analytically. Besides the edge local flattening of the safety factor and local sharp pressure gradients [25], the short wavelength (viz. high-m) modes suppression is achieved by the combined effect of poloidal MHD and ion diamagnetic flow, which forces the total ion poloidal rotation to be zero. A vacuum gap between plasma and the metallic wall is necessary, though its effect is weakened for sufficiently large m and reduced by the presence of the separatrix. Although highly simplified profiles for pressure, mass density and equilibrium rotation have been employed, all features measured experimentally and modelled numerically have been retrieved. These are: (i) the strong dependence of the EHO appearance on the $\boldsymbol{E} \times \boldsymbol{B}$ poloidal rotation letting low-n modes emerge, (ii) the independence of the growth rate upon the sign of the toroidal flow [17, 19, 44], (iii) the rotation frequency spacing of the toroidal harmonics close to the plasma toroidal rotation (if sufficiently large) at the pedestal top [3, 10, 13] and (iv) the pedestal localised structure of the radial eigenfunction.

This work has been carried out within the framework of the EUROfusion Consortium and has received funding from the Euratom research and training programme 2014-2018 under grant agreement No 633053. The views and opinions expressed herein do not necessarily reflect those of the European Commission. This work was supported in part by the Swiss National Science Foundation.

* Electronic address: brunetti@ifp.cnr.it

[1] F. Wagner, Plasma Phys. Control. Fusion **49**, B1 (2007).
[2] A. W. Leonard, Phys. Plasmas **21**, 090501 (2014).
[3] C. M. Greenfield *et al.*, Phys. Rev. Lett. **86**, 4544 (2001).
[4] K. H. Burrell *et al.*, Plasma Phys. Control. Fusion **44**, A253 (2002).
[5] W. Suttrop *et al.*, Plasma Phys. Control. Fusion **45**, 1399 (2003).
[6] K. H. Burrell *et al.*, Phys. Plasmas **12**, 056121 (2005).
[7] X. Chen *et al.*, Nucl. Fusion **56**, 076011 (2016).
[8] K. H. Burrell *et al.*, Phys. Plasmas **8**, 2153 (2001).
[9] W. Suttrop *et al.*, Nucl. Fus. **45**, 721 (2005).
[10] E. R. Solano *et al.*, Phys. Rev. Lett. **104**, 185003 (2010).
[11] N. Oyama *et al.*, Nucl. Fus. **45**, 871 (2005).
[12] K. H. Burrell *et al.*, Nucl. Fus. **49**, 085024 (2009).
[13] L. J. Zheng *et al.*, Nucl. Fusion **53**, 063009 (2013).
[14] S. Y. Medvedev *et al.*, Plasma Phys. Control. Fusion **48**, 927 (2006).
[15] L. J. Zheng *et al.*, Phys. Plasmas **20**, 012501 (2013).
[16] G. Q. Dong *et al.*, Phys. Plasmas **24**, 112510 (2017).
[17] F. Liu *et al.*, Nucl. Fus. **55**, 113002 (2015).
[18] J. R. King *et al.*, Phys. Plasmas **24**, 055902 (2017).
[19] A. M. Garofalo *et al.*, Nucl. Fus. **51**, 083018 (2011).
[20] F. Liu *et al.*, Plasma Phys. Control. Fusion **60**, 014039 (2018).
[21] W. A. Cooper *et al.*, J. Plasma Phys. **81**, 515810605 (2015).
[22] W. A. Cooper *et al.*, Plasma Phys. Control. Fusion **58**, 064002 (2016).
[23] W. A. Cooper *et al.*, Phys. Plasmas **23**, 040701 (2016).
[24] A. Kleiner *et al.*, Nucl. Fus. **58**, 074001 (2018).
[25] D. Brunetti *et al.*, Nucl. Fus. **58**, 014002 (2018).
[26] D. Brunetti *et al.*, Plasma Phys. Control. Fusion **56**, 075025 (2014).
[27] R. D. Hazeltine and J. D. Meiss, *Plasma Confinement* (Addison-Wesley Publishing Company, Redwood City, 1992).
[28] A. M. Garofalo *et al.*, Phys. Plasmas **22**, 056116 (2015).
[29] Note that $v^\varphi = \boldsymbol{v} \cdot \boldsymbol{\nabla}\varphi$ has the dimensions of a frequency. Same argument applies to v^ϑ.
[30] C. Wahlberg *et al.*, Plasma Phys. Control. Fusion **55**, 105004 (2013).
[31] R. J. Hastie and T. C. Hender, Nucl. Fusion **28**, 585 (1988).

[32] C. G. Gimblett *et al.*, Phys. Plasmas **3**, 33691 (1996).
[33] W. Newcomb, Ann. Phys. **10**, 232 (1960).
[34] E. Frieman and M. Rotenberg, Rev. Mod. Phys. **32**, 898 (1960).
[35] Z. B. Guo and P. H. Diamond, Phys. Rev. Lett. **114**, 145002 (2015).
[36] E. Viezzer *et al.*, Nucl. Fus. **53**, 053005 (2013).
[37] B. Coppi *et al.*, Nucl. Fus. **6**, 101 (1966).
[38] A. B. Mikhailovskii, *Instabilities in a Confined Plasma* (IOP, Bristol, 1998).
[39] A. B. Mikhailovskii *et al.*, Nucl. Fus. **13**, 259 (1973).
[40] J. W. Havenkort and H. J. de Blank, Phys. Rev. E **86**, 016411 (2012).
[41] A. H. Glasser *et al.*, Phys. Fluids **18**, 875 (1975).
[42] We assume that $\Omega(r_p) = \Omega(r_1)$ and $\rho_0(r_p) = \rho_0(r_1)$.
[43] H. J. de Blank and T. J. Schep, Phys. Fluids B **3**, 1136 (1991).
[44] K. H. Burrell *et al.*, Phys. Rev. Lett. **102**, 155003 (2009).